Electron-hole liquid in many-band systems. I. Ge and Si under large uniaxial strain*

P. Vashishta
Argonne National Laboratory, Argonne, Illinois 60439

P. Bhattacharyya† and K. S. Singwi
Physics Department, Northwestern University, Evanston, Illinois 60201
and Argonne National Laboratory, Argonne, Illinois 60439

(Received 23 October 1973)

The ground-state energy of a quantum electron-hole liquid in the three cases (i) a single isotropic maximum for the hole band and a single minimum for the conduction band (called the model system), (ii) Ge under a large [111] strain, and (iii) Si under a large [100] strain, has been calculated in the random-phase (RPA), Hubbard (HA), and fully-self-consistent (FSC) approximations. The last approximation takes into account multiple scatterings to infinite order between all components of the plasma. Effects of anisotropy of bands have also been fully considered. Besides the ground-state energy, we have also calculated the partial-pair-correlation functions and enhancement factors. For the model system, calculations have also been made for different mass ratios. Two important results of this paper are (i) the electron-hole liquid in both Ge and Si under a large uniaxial strain should exhibit a metallic phase relative to a free excitonic phase. The calculated binding energies for Ge[111] and Si[100] are, respectively, 4.9 °K and 21.8 °K, corresponding to equilibrium densities of 1.11×10^{16} and 4.47×10^{17} cm^{-3}. (ii) The enhancement factors at the equilibrium density for Ge[111] and Si[100] are, respectively, 6.8 and 7.4. We suggest that experiments should be done to test these predictions of the FSC theory because of their bearing on the validity of different many-body approximations.

I. INTRODUCTION

It was first suggested by Keldysh[1] that nonequilibrium electrons and holes in Ge and Si, generated under high excitation power, would undergo a gas-liquid-type transition at low temperatures as a function of density. That such a transition does indeed occur has now been demonstrated by a variety of experiments.[2-18] These experiments furnish us for the first time with a quantitative measure of the ground-state energy and equilibrium density for the degenerate electron-hole plasma—a situation which is quite unique. Moreover, we have here a system whose characteristics, in contrast to the metallic case, are known exactly. For these reasons, the theoretical problem of calculating the ground-state energy of the system becomes very interesting. It provides an opportunity to test unambiguously the validity of different many-body approximations that are used in the calculation.

Ground-state energy calculations, including many-body effects, of the electron-hole liquid in ordinary Ge and Si have recently been reported by Hanamura,[19] Brinkman *et al.*[20] (BRAC), and Brinkman and Rice[21] (BR) and independently by Combescot and Nozières[22] (CN). The basic theoretical approach of the latter two groups of authors is equivalent in principle, although they differ in detail such as the consideration of anisotropy and degeneracy of hole bands in the calculation of the correlation part of the ground-state energy. BRAC use the Hubbard approximation[23] as generalized to a many-component plasma. The Hubbard approximation takes only exchange effects into account, and, as we know from our experience of the electron-gas case, it is a fairly good approximation for not too low densities. CN, on the other hand, use the Nozières-Pines interpolation scheme,[24] which is exact in the two limiting cases of small and large wave numbers. We shall not dwell here on the merits of these and other approximations since they have been discussed at great length for the electron gas by Singwi *et al.*[25] in a series of papers. The energy minima and the equilibrium densities as calculated by BR and CN both in Ge and Si are in reasonably good agreement with the available experimental data.[26] The results of CN should be more trustworthy, since they have properly treated effects of anisotropy and valence band coupling.

In the above-mentioned calculations, an important effect of multiple electron-hole scattering has been completely neglected, and it has not been found possible in the formulation of these authors to take this effect into account. At the same time we know that it is the multiple scattering which in the very-low-density limit is ultimately responsible for the excitonic phase. But since the calculations[20-22] already give lower values for the binding energy compared with experiment, one is led to to believe that the effect of multiple scattering, at least in the region of densities of interest ($r_s \simeq 0.6$ in Ge and 0.9 in Si), is very small if not negligible.

This, however, needs to be examined quantitatively. On the other hand, in a recent experimental paper Benoît à la Guillaume and Voos[27] point out that at the present time there is a real discrepancy between experiment and theory (BR) as regards the value of the enhancement factor $g_{eh}(0)$, the ratio of the electron density on the hole to the mean density. They estimate $g_{eh}(0)$ to be less than 12 but much greater than 2, the latter value being the estimate of BR. If the experimental estimate of $g_{eh}(0)$ is to be trusted, it would imply, as these authors also suggest, a substantial contribution from electron-hole scattering, a result in direct contradiction to what is dictated by the ground-state energy calculation. The only way to settle these questions is to incorporate the effect of multiple scattering in the theory. The complexity of the band structure of Ge and Si makes a numerical calculation of the ground-state energy with multiple scattering almost prohibitive to handle, even on a fast computer. To make such a calculation feasible one has to resort to approximate schemes.

Fortunately, the band structure of Ge and Si is considerably simplified under a large uniaxial strain.[28] In the limit of infinite strain, in each case one deals with a single valence band, but while for Ge[111] one has only a single conduction band, for Si[100] one has two. In this paper we shall be concerned with the calculation of the ground-state energy of the electron-hole liquid in strained Ge[111] and Si[100].[29] As we shall see, both these systems are very interesting. Brinkman and Rice[21] have calculated the ground-state energy of Ge under a large uniaxial [111] strain within the Hubbard approximation. They find that the metallic phase is bound by such a small amount that in view of the uncertainties inherent in the Hubbard approximation no definite theoretical conclusion as to the existence of this phase can be reached. On the other hand, Combescot and Nozières[22] find no binding within their interpolation scheme, which is supposed to be somewhat better than the Hubbard approximation. Experimentally,[28] recombination radiation of the condensed phase both in strained Ge and Si has been observed, although no definite values of the energy minima and the equilibrium densities have been given.

In these experiments it is not certain whether one has reached the limit of infinite strain. Under very large strain, one could even be skeptical about the very existence of a metallic phase. It is at least clear from the calculations of both BR and CN that, if a metallic phase occurs at all in highly strained Ge and Si, it will occur for a value of $r_s \approx 1.5$. This value of r_s is much greater than that for ordinary Ge and Si. The effect of multiple scattering on the calculation of the ground-state energy for such densities turns out to be very important, and as we shall see it is responsible for metallic binding in these systems.

It seems appropriate here to comment briefly on the mathematical formulation which we shall employ for our calculations. The formulation is based on the theory of electron correlations of Singwi *et al.*, as generalized to a many-component plasma. Such a generalization to a two-component system consisting of a degenerate electron and a few positrons was first made by Sjölander and Stott[30] and later extended by Bhattacharyya and Singwi.[31] The merit of this formulation consists in the fact that it is self-consistent and treats both exchange and Coulomb correlations better than previous theories and takes multiple scattering between components into account to infinite order, although in an approximate way. Random-phase and Hubbard approximations are special cases of this formulation. That our self-consistent scheme is a definite improvement over the random phase and Hubbard approximations for a single-component case (electrons at metallic densities) has been demonstrated before. Since, within the framework of this scheme, it has been found possible to account satisfactorily for the positron annihilation rates[31] in the metallic-density range, it is an indication of the fact that multiple scattering is being treated satisfactorily. Also, using this formulation, it has been shown[32] that the correlation energy of a positron in an electron gas approaches smoothly, as a function of r_s, to the binding energy of a positronium. These facts, together with others, give us some confidence when we apply the self-consistent scheme to a multicomponent quantum plasma.

This paper is divided into several sections. In Sec. II we outline briefly our self-consistent scheme as generalized to a two-component degenerate plasma of electron and holes, and give formulas for various response functions. Special cases of the random phase, Hubbard, and self-consistent particle-hole approximations are discussed.

In Sec. III we give the formulas for the Hartree-Fock and correlation energies for the isotropic and anisotropic bands. Section IV outlines the procedure for calculations and in Sec. V we give our results. In the same section, a detailed discussion of the ground-state energy, partial-pair-correlation functions [$g_{ee}(\vec{r})$, $g_{eh}(\vec{r})$, and $g_{hh}(\vec{r})$], and the enhancement factor $g_{eh}(0)$ for the model system in different approximations is given. A similar discussion is given for highly strained Ge[111] and Si[100]. One of the two important results of this paper is that within the framework of

our self-consistent theory we are able to predict that both Ge and Si under a large uniaxial strain should exhibit a metallic state relative to free excitons. The other important result is that the enhancement factors in both Ge[111] and Si[100] are nearly three times as large as those obtained in the Hubbard approximation. In the concluding Sec. VI, we suggest that experiments should be done to verify our predictions.

II. TWO-COMPONENT DEGENERATE PLASMA

We consider a neutral two-component degenerate plasma consisting of electrons and holes. In the absence of any external disturbance, the dynamics of the system is governed by the Hamiltonian H_0 consisting of kinetic and Coulomb energies. We now apply a weak external potential $V^i_{\rm ext}(\vec{x}, t)$ which acts only on the ith component of the plasma. The dynamics are then governed by the Hamiltonian

$$H = H_0 + \sum_i \int e_i n_i(\vec{x}, t) V^i_{\rm ext}(\vec{x}, t)\, d\vec{x} , \tag{1}$$

where e_i is the charge on the ith-type particles and n_i the corresponding density.

Following the linear response theory,[33] we can write the induced density in the ith component as

$$\langle\langle \delta n_i(\vec{q}, \omega)\rangle\rangle = \sum_{j=1}^{2} \chi_{ij}(\vec{q}, \omega) V^j_{\rm ext}(\vec{q}, \omega) , \tag{2}$$

where $\delta n_i(\vec{q}, \omega)$ and $V^j_{\rm ext}(\vec{q}, \omega)$ are, respectively, the Fourier transforms of $\delta n_i(\vec{x}, t)$ and $V^j_{\rm ext}(\vec{x}, t)$, and $\chi_{ij}(\vec{q}, \omega)$ is the density-density response function.

In the spirit of the generalized random-phase approximation, we write

$$\langle\langle \delta n_1(\vec{q}, \omega)\rangle\rangle = \chi^1_0(\vec{q}, \omega)[V^1_e(\vec{q}, \omega) + \psi_{11}(\vec{q})\langle\langle \delta n_1(\vec{q}, \omega)\rangle\rangle + \psi_{12}(\vec{q})\langle\langle \delta n_2(\vec{q}, \omega)\rangle\rangle] \tag{3a}$$

and

$$\langle\langle \delta n_2(\vec{q}, \omega)\rangle\rangle = \chi^2_0(\vec{q}, \omega)[V^2_e(\vec{q}, \omega) + \psi_{21}(\vec{q})\langle\langle \delta n_1(\vec{q}, \omega)\rangle\rangle + \psi_{22}(\vec{q})\langle\langle \delta n_2(\vec{q}, \omega)\rangle\rangle] , \tag{3b}$$

where $\chi^i_0(\vec{q}, \omega)$ is the noninteracting polarizability[34] of the ith component and $\psi_{ij}(\vec{q})$ is the static effective interaction between the components i and j. The set of Eqs. (3) can be trivially solved to give explicit expressions for $\langle\langle \delta n_i(\vec{q}, \omega)\rangle\rangle$,

$$\langle\langle \delta n_1(\vec{q}, \omega)\rangle\rangle = \frac{\chi^1_0(\vec{q}, \omega)[1 - \chi^2_0(\vec{q}, \omega)\psi_{22}(\vec{q})] V^1_{\rm ext}(\vec{q}, \omega)}{\Delta(\vec{q}, \omega)} + \frac{\chi^1_0(\vec{q}, \omega)\chi^2_0(\vec{q}, \omega)\psi_{21}(\vec{q}) V^2_{\rm ext}(\vec{q}, \omega)}{\Delta(\vec{q}, \omega)} , \tag{4}$$

where

$$\Delta(\vec{q}, \omega) = [1 - \chi^1_0(\vec{q}, \omega)\psi_{11}(\vec{q})][1 - \chi^2_0(\vec{q}, \omega)\psi_{22}(\vec{q})] - \chi^1_0(\vec{q}, \omega)\psi_{12}(\vec{q})\chi^2_0(\vec{q}, \omega)\psi_{21}(\vec{q}) . \tag{5}$$

The equation for $\langle\langle \delta n_2(\vec{q}, \omega)\rangle\rangle$ follows by interchanging the indices 1 and 2 in Eq. (4).

A comparison of Eq. (4) with Eq. (2) gives the response functions

$$\chi_{11}(\vec{q}, \omega) = \frac{\chi^1_0(\vec{q}, \omega)[1 - \chi^2_0(\vec{q}, \omega)\psi_{22}(\vec{q})]}{\Delta(\vec{q}, \omega)} ,$$

$$\chi_{12}(\vec{q}, \omega) = \frac{\chi^1_0(\vec{q}, \omega)\chi^2_0(\vec{q}, \omega)\psi_{21}(\vec{q})}{\Delta(\vec{q}, \omega)} , \tag{6}$$

$$\chi_{22}(\vec{q}, \omega) = \frac{\chi^2_0(\vec{q}, \omega)[1 - \chi^1_0(\vec{q}, \omega)\psi_{11}(\vec{q})]}{\Delta(\vec{q}, \omega)} .$$

It follows simply from the symmetry that $\psi_{21}(\vec{q}) = \psi_{12}(\vec{q})$ and $\chi_{21}(\vec{q}, \omega) = \chi_{12}(\vec{q}, \omega)$.

So far we have discussed the formalism for a two-component plasma as applicable to the model system and Ge[111]. In Appendix I we give the expressions for the response functions $\chi_{ij}(\vec{q}, \omega)$ for a three-component system, as is the case in Si[100].

In general, the effective potential $\psi_{ij}(\vec{q})$ defines a local field correction in terms of the "bare" Coulomb potential $\varphi_{ij}(\vec{q}) = 4\pi e_i e_j/\kappa q^2$, where κ is the static dielectric constant of the medium:

$$\psi_{ij}(\vec{q}) = \varphi_{ij}(\vec{q})[1 - G_{ij}(\vec{q})] . \tag{7}$$

Approximations, which go under different names, to the response functions in Eq. (6) are indeed the approximations for $G_{ij}(\vec{q})$.

The elements $\epsilon_{ij}(\vec{q}, \omega)$ of the dielectric tensor are defined in terms of the elements $\chi_{ij}(\vec{q}, \omega)$ by

$$\frac{1}{\epsilon_{ij}(\vec{q}, \omega)} - \delta_{ij} = \varphi_{ij}(\vec{q})\chi_{ij}(\vec{q}, \omega) , \tag{8}$$

$$\frac{1}{\epsilon(\vec{q}, \omega)} - 1 = \sum_{ij}\left(\frac{1}{\epsilon_{ij}(\vec{q}, \omega)} - \delta_{ij}\right) . \tag{9}$$

A. Random-phase approximation (RPA)

In RPA, $G_{ij}(\vec{q}) = 0$ and therefore $\psi_{ij}(\vec{q}) = \varphi_{ij}(\vec{q})$. Using Eqs. (6) and (8), Eq. (9) becomes

$$\epsilon(\vec{q}, \omega) = 1 - \varphi(\vec{q})\chi^1_0(\vec{q}, \omega) - \varphi(\vec{q})\chi^2_0(\vec{q}, \omega) , \tag{10}$$

where $\varphi(\vec{q}) = 4\pi e^2/\kappa q^2$. Thus in RPA, $\epsilon(\vec{q}, \omega)$ has a very simple form. Extension of Eq. (10) to a system with more than two components is obvious. From Eq. (10) it follows that the square of the plasma frequency of the two-component plasma is equal to the sum of the squares of the individual plasma frequencies.

B. Hubbard approximation (HA)

This approximation is characterized by

$$G_{ij}(\vec{q}) = \tfrac{1}{2}[q^2/(q^2 + q^2_{Fi})]\delta_{ij} , \tag{11}$$

where q_{Fi} is the Fermi wave vector of the ith component. The HA takes exchange into account and

corresponds to the case where the Pauli hole is used in calculating the local-field correction between the particles of the same species. No Coulomb correlations are included. In this approximation it is straightforward to show that

$$\epsilon(\vec{q},\omega)=1-\varphi(\vec{q})\sum_{i=1}^{2}\frac{\chi_0^i(\vec{q},\omega)}{1+\varphi(\vec{q})G_{ii}(\vec{q})\chi_0^i(\vec{q},\omega)}\ . \quad (12)$$

Equation (12) justifies the procedure of BR when they generalize the Hubbard approximation to multicomponent plasma.

C. Fully-self-consistent (FSC) approximation

In the approximation of Singwi *et al.*,[25] $G_{ij}(\vec{q})$ is given by

$$G_{ij}(\vec{q})=-\frac{1}{n}\int\frac{\vec{q}\cdot\vec{q}'}{q'^2}\gamma_{ij}(\vec{q}-\vec{q}')\frac{d\vec{q}'}{(2\pi)^3}\ , \quad (13)$$

where n is the number density of electrons and the structure factor $\gamma_{ij}(\vec{q})$ is related to the partial-pair-correlation function $g_{ij}(\vec{r})$ as

$$g_{ij}(\vec{r})-1=\frac{1}{n}\int\frac{d\vec{q}}{(2\pi)^3}\,e^{i\vec{q}\cdot\vec{r}}\gamma_{ij}(\vec{q})\ . \quad (14)$$

The fluctuation-dissipation theorem[35] in a multicomponent case is

$$\langle n_{\vec{q}}^i n_{-\vec{q}}^j\rangle=\Omega n_i\left(\delta_{ij}+\frac{n_j}{n}\gamma_{ij}(\vec{q})\right)$$
$$=-\frac{\Omega\hbar}{\pi}\int_0^\infty d\omega\,\mathrm{Im}\chi_{ij}(q,\omega)\ . \quad (15)$$

In this approximation Eqs. (13), (15), and (6) have to be solved self-consistently. In a two component case, which we are considering here, we have three simultaneous linear integral equations, one for each $\gamma_{11}(\vec{q})$, $\gamma_{12}(\vec{q})$, and $\gamma_{22}(\vec{q})$ to be solved self-consistently. The number of such equations increases rapidly as the number of components in the plasma increases, thus making a FSC solution of the problem very time consuming, even on a fast computer.

D. Self-consistent particle-hole (SPH) approximation

As mentioned before, the FSC approximation becomes impracticable when one is dealing with multicomponent plasmas, as in normal Ge and Si. One is therefore forced to devise a further approximation to handle such problems. The approximation that we have tried and tested numerically is what we call SPH. It consists in choosing (say in a two-component case)

$$G_{12}(\vec{q})=-\frac{1}{n}\int\frac{\vec{q}\cdot\vec{q}'}{q'^2}\gamma_{12}(\vec{q}-\vec{q}')\frac{d\vec{q}'}{(2\pi)^3} \quad (16)$$

and

$$G_{ii}(\vec{q})=\tfrac{1}{2}q^2/(q^2+q_{Fi}^2)\ . \quad (17)$$

In essence, here one uses the Hubbard approximation between particles of the same species and takes electron-hole multiple scattering in the spirit of the FSC approximation. Thus, in contrast to the FSC approximation, where we have three equations to be solved, in SPH approximation there is only one equation for $\gamma_{12}(\vec{q})$ to be solved self-consistently. The RPA, Hubbard, and SPH approximations discussed above are special cases of the FSC approximation. We shall discuss this approximation in detail in another paper dealing with normal Ge and Si.

III. GROUND-STATE ENERGY

The ground-state energy E_0 is the sum of (i) kinetic, (ii) exchange, and (iii) correlation parts. The first two contributions, called the Hartree-Fock energy, can be calculated exactly, whereas the last one can only be calculated in an approximate scheme. Relative merits of the approximations mentioned in Secs. II A–II C in the calculation of the correlation energy have been discussed in detail for one-component plasma by Singwi *et al.*[25] In a multi-component plasma the superiority of this FSC approximation over the others lies in the fact that it takes multiple scattering between electron and holes into account to all orders in an approximate way and yields physically acceptable partial-pair distribution functions.

We shall in what follows adopt appropriate reduced units, in line with earlier authors.[22,23] All wave vectors are measured in units of the wave vector K_0, which is related to the number density of electrons n through

$$K_0=(3\pi^2 n)^{1/3}\ . \quad (18)$$

Energy is measured in units of excitonic rydberg

$$E_x=\mu e^4/2\hbar^2\kappa^2=e^2/2\kappa a_x\ , \quad (19)$$

where the reduced mass μ is

$$1/\mu=1/m_{oe}+1/m_{oh}\ , \quad (20)$$

where m_{oe} and m_{oh} are, respectively, the optical masses of the electron and the hole, which in turn are defined in terms of the longitudinal mass m_l and the transverse mass m_t by

$$1/m_o=\tfrac{1}{3}(1/m_l+2/m_t)\ . \quad (21)$$

In Eq. (19) a_x is the excitonic Bohr radius defined by

$$a_x=\kappa\hbar^2/\mu e^2\ . \quad (22)$$

The usual dimensionless parameter r_s is defined by

$$r_s=(\tfrac{9}{4}\pi)^{1/3}/K_0 a_x\ . \quad (23)$$

A. Hartree-Fock (HF) energy

The kinetic and exchange energies per electron-hole (e-h) pair, for a system of ν conduction bands and one valence band, in excitonic rydbergs, are given by[22]

$$\frac{T}{N}=\frac{2.2099}{r_s^2}\left(\frac{\mu}{\nu^{2/3}m_{de}}+\frac{\mu}{m_{dh}}\right)\text{Ry}\,, \tag{24}$$

$$\frac{E_{ex}}{N}=\frac{0.9163}{r_s}\left[\nu^{-1/3}\varphi(\rho_e)+\varphi(\rho_h)\right]\text{Ry}\,, \tag{25}$$

where the function $\varphi(\rho)$ is given by

$$\varphi(\rho)=\rho^{1/6}\left(\frac{\sin^{-1}[(1-\rho)^{1/2}]}{(1-\rho)^{1/2}}\Theta(1-\rho)+\frac{\sinh^{-1}[(\rho-1)^{1/2}]}{(\rho-1)^{1/2}}\Theta(\rho-1)\right) \tag{26}$$

and

$$\rho\equiv m_t/m_l\,. \tag{27}$$

$\Theta(\rho)$ is the usual step function and N is the number of e-h pairs. In Eq. (24), m_d is the density-of states mass, which is given by

$$m_d=(m_l m_t^2)^{1/3}\,. \tag{28}$$

For the isotropic electron-hole bands, $\rho^e=\rho^h=1$ and $\varphi(\rho)=1$, the HF energy per pair is

$$\frac{E_{HF}}{N}=\epsilon_{HF}=\frac{2.2099}{r_s^2}-\frac{1.8326}{r_s}\ \text{Ry, model}\,. \tag{29}$$

For Ge[111] and Si[100], using the parameters[36] given in Tables I and II, which are the same as used by BR, the HF energy per e-h pair in excitonic rydbergs is determined to be[29]

$$\epsilon_{HF}=\frac{1.6180}{r_s^2}-\frac{1.6594}{r_s}\ \text{Ry, Ge[111]}\,, \tag{30}$$

$$\epsilon_{HF}=\frac{1.6846}{r_s^2}-\frac{1.6052}{r_s}\ \text{Ry, Si[100]}\,. \tag{31}$$

B. Correlation energy

For a multicomponent system interacting via the Coulomb law, the interaction Hamiltonian $\mathcal{H}_{int}$ is

$$\mathcal{H}_{int}(\vec{q},\lambda)=\frac{\lambda}{2\Omega}\sum_{ij}\frac{4\pi e_i e_j}{\kappa q^2}(n_{\vec{q}}^i n_{-\vec{q}}^j-N_i^{op}\delta_{ij})\,, \tag{32}$$

and hence the interaction energy is

$$E_{int}(\lambda)=\frac{\lambda}{2\Omega}\sum_{ij}\sum_{\vec{q}}\frac{4\pi e_i e_j}{\kappa q^2}(\langle n_{\vec{q}}^i n_{-\vec{q}}^j\rangle-N_i\delta_{ij})\,, \tag{33}$$

where N_i is the number of particles in the ith component and λ is the interaction parameter.[37] The density-density correlation in Eq. (33) is given as

$$\langle n_{\vec{q}}^i n_{-\vec{q}}^j\rangle=N_i[\delta_{ij}+(n_j/n)\gamma_{ij}(\vec{q})]\,, \tag{34}$$

where the first term on the right-hand side arises from the self-part of the density-density correlation function. Using Eq. (34) in Eq. (33) we can write

$$E_{int}(\lambda)=\frac{\lambda N}{2\Omega}\sum_{\vec{q}}\frac{4\pi e^2}{\kappa q^2}\sum_{ij}\xi_i\xi_j\frac{n_i n_j}{n^2}\gamma_{ij}(\vec{q})\,, \tag{35}$$

where $\xi_i=+1,-1$ for holes and electrons, respectively. Defining a quantity

$$\gamma(\vec{q})=\sum_{ij}\xi_i\xi_j\frac{n_i n_j}{n^2}\gamma_{ij}(\vec{q})\,, \tag{36}$$

Eq. (35) can now be written

$$E_{int}(\lambda)=\frac{\lambda N}{2\Omega}\sum_{\vec{q}}\frac{4\pi e^2}{\kappa q^2}\gamma(\vec{q})\,. \tag{37}$$

The above expression is now similar in form to the corresponding expression for one-component plasma.[25] Proceeding in an analogous manner, we have

$$\frac{dE_{int}(\lambda)}{d\lambda}=\frac{E_{int}(\lambda)}{\lambda}=\frac{N}{2\Omega}\sum_{\vec{q}}\frac{4\pi e^2}{\kappa q^2}\gamma(\vec{q},\lambda)\,. \tag{38}$$

The interaction energy per e-h pair is therefore

$$\epsilon_{int}=\frac{1}{N}\int_0^1\frac{d\lambda}{\lambda}E_{int}(\lambda)=\tfrac{1}{2}\int_0^1 d\lambda\int\frac{d\vec{q}}{(2\pi)^3}\frac{4\pi e^2}{\kappa q^2}\gamma(\vec{q},\lambda)\,. \tag{39}$$

We can now change over[38] to an integration over r_s' by using

$$K_0 r_s'\kappa\hbar^2/\mu e^2\lambda=(\tfrac{9}{4}\pi)^{1/3}=1/\alpha\,. \tag{40}$$

Using Eq. (40), Eq. (39) becomes

$$\epsilon_{int}=-\frac{2}{\pi}\frac{\alpha\hbar^2}{\mu}K_0^2\int_0^{r_s}dr_s'\times\left(-\frac{1}{2}\int_0^\infty dQ\int_0^1 d\mu\,\gamma(Q,\mu,r_s')\right)\,, \tag{41}$$

where $Q=q/K_0$. Defining

$$\bar{\gamma}(r_s')=-\tfrac{1}{2}\int_0^\infty dQ\int_0^1 d\mu\,\gamma(Q,\mu,r_s')\,, \tag{42}$$

and using Eqs. (19), (22), and (23), Eq. (41) becomes

TABLE I. Table of constants for Si and Ge. The form of the energy eigenvalue is $E^{\pm}(\vec{k})=Ak^2\pm[B^2k^4+C^2(k_x^2k_y^2+k_y^2k_z^2+k_z^2k_x^2)]^{1/2}$. The values of A, B, and C are taken from the latest cyclotron-resonance work of Hensel and Suzuki, Ref. 36.

	A	B	C	κ
Si	4.28	0.75	4.85	11.4
Ge	13.38	8.48	13.15	15.36

$$\epsilon_{\rm int} = -\frac{4}{\pi\alpha r_s^2}\int_0^{r_s}\bar{\gamma}(r_s')\,dr_s' \text{ Ry} . \tag{43}$$

Correlation energy by definition is $\epsilon_{\rm int}$ minus the exchange energy, and therefore

$$\epsilon_{\rm corr} = \frac{-4}{\pi\alpha r_s^2}\int_0^{r_s}\bar{\gamma}(r_s')\,dr_s' - \epsilon_{\rm ex} \text{ Ry} , \tag{44}$$

where $\epsilon_{\rm ex}$ is given by Eq. (25).

IV. CALCULATIONS

In this section we shall briefly outline our procedure for performing numerical calculations. For simplicity, we give an explicit discussion for the two-component case only. The relevant formulas are given in dimensionless form. Throughout this section the frequency ω and wave vectors q are expressed in units of $\hbar K_0^2/2\mu$ and K_0, respectively.

Equations (13), (6), and (15) constitute the basic equations of this paper. For a two-component plasma the three equations for $\gamma_{11}(\vec{q})$, $\gamma_{12}(\vec{q})$, and $\gamma_{22}(\vec{q})$ have to be solved self-consistently in the FSC approximation. RPA, Hubbard and SPH approximations are the limiting cases of FSC approximation. Equations (5) and (6) can be written in the dimensionless form as

$$N_{11}(\vec{q},\omega)\Delta^{-1}(\vec{q},\omega) = -\varphi(q)\chi_{11}(\vec{q},\omega) = Q_1^0[1+Q_2^0(1-G_{22})]\Delta^{-1}(\vec{q},\omega) , \tag{45}$$

$$N_{12}(\vec{q},\omega)\Delta^{-1}(q,\omega) = \varphi(q)\chi_{12}(\vec{q},\omega) = Q_1^0 Q_2^0(1-G_{12})\Delta^{-1}(\vec{q},\omega) , \tag{46}$$

and

$$\Delta(\vec{q},\omega) = [1+(1-G_{11})Q_1^0][1+(1-G_{22})Q_2^0] - (1-G_{12})^2 Q_1^0 Q_2^0 . \tag{47}$$

Similarly, the expression for $N_{22}(\vec{q},\omega)$ can be written by interchanging 1 and 2 in N_{11} in Eq. (45). $Q_i^0(\vec{q},\omega) = -\varphi(q)\chi_0^i(\vec{q},\omega)$ is the usual Lindhard function.[34] In the isotropic situation, the real and imaginary parts of $Q_i^0(\vec{q},\omega)$, for the ith plasma component whose density is n_i and particle mass is m_i, can be written

$$\mathrm{Re}Q_i^0(q,\omega) = \frac{K^2}{q^2}\left(\frac{\delta_i}{\beta_i}\right)\left\{\frac{1}{2}+\frac{\delta_i}{4q}\left[1-\left(\frac{\omega+\beta_i q^2}{2\beta_i\delta_i q}\right)^2\right]\ln\left|\frac{\omega+2\beta_i\delta_i q+\beta_i q^2}{\omega-2\beta_i\delta_i q+\beta_i q^2}\right| + \frac{\delta_i}{4q}\left[1-\left(\frac{\omega-\beta_i q^2}{2\beta_i\delta_i q^2}\right)^2\right]\ln\left|\frac{\omega-2\beta_i\delta_i q-\beta_i q^2}{\omega+2\beta_i\delta_i q-\beta_i q^2}\right|\right\} \tag{48}$$

$$\mathrm{Im}Q_i^0(q,\omega) = \frac{\pi}{4}\frac{K^2}{\beta_i}\frac{\omega}{\beta_i q^3} \qquad \omega \le \beta_i(2\delta_i q - q^2)$$
$$= \frac{\pi}{4}\frac{K^2}{\beta_i}\frac{\delta_i^2}{q^3}\left[1-\left(\frac{\omega-\beta_i q^2}{2\beta_i\delta_i q}\right)^2\right] \qquad |\beta_i(2\delta_i q - q^2)| \le \omega \le |\beta_i(2\delta_i q + q^2)| \tag{49}$$
$$= 0, \quad \omega \ge \beta_i(2\delta_i q + q^2) ,$$

where $K^2 = 4\mu e^2/\pi\hbar^2 K_0\kappa$, $\beta_i = \mu/m_i$, and $\delta_i = q_{\rm Fi}/K_0$. Recall that in the present case $m_i \equiv m_{oi}$. The local field $G_{ij}(\vec{q})$ in Eq. (13) becomes

$$G_{ij}(q) = -\frac{3}{4}\int_0^\infty q'^2\gamma_{ij}(q')\left(1+\frac{q^2-q'^2}{2qq'}\ln\left|\frac{q+q'}{q-q'}\right|\right)dq' . \tag{50}$$

TABLE II. Values of constants used in the calculations for Ge[111] and Si[100]. The masses are given in units of the bare electron mass. m_{de}, m_{dh} = density-of-states masses for electron and hole. m_{0e}, m_{0h} = optical masses for electron and hole bands. $\mu_0 \equiv \mu$ = reduced optical mass of electron and hole. E_x = excitonic rydberg. $m_{hl}^{-1} = A + \frac{1}{3}(3C^2+9B^2)^{1/2}$ and $m_{ht}^{-1} = A - \frac{1}{6}(3C^2+9B^2)^{1/2}$ (Ge[111][36]). $m_{h1}^{-1} = A+B$ and $m_{ht}^{-1} = A - \frac{1}{2}B$ (Si[100][36]).

	m_{el}	m_{et}	m_{de}	m_{oe}	m_{hl}	m_{ht}	m_{dh}	m_{oh}	μ_0	E_x (meV)
Ge[111]	1.580	0.082	0.2198	0.120	0.040	0.130	0.088	0.075	0.046	2.65
Si[100]	0.9163	0.1905	0.3216	0.2588	0.154	0.523	0.2354	0.2336	0.1228	12.85

The fluctuation-dissipation theorem can be written

$$\gamma_{ij}(\vec{q})=\frac{3q^2}{2\pi K^2}\frac{n^2}{n_i n_j}\int_{\text{single-particle-hole continuum}} d\omega\,\mathrm{Im}\left(\frac{N_{ij}(\vec{q},\omega)}{\Delta(\vec{q},\omega)}\right)+\frac{3}{2}\frac{q^2}{K^2}\left(\frac{n^2}{n_i n_j}\right)\left(-\frac{\mathrm{Re}N_{ij}(\vec{q},\omega)}{\mathrm{Re}\Delta'(\vec{q},\omega)}\right)_{\omega=\omega_p}-\left(\frac{n}{n_j}\right)\delta_{ij}\,, \tag{51}$$

where we have written explicitly the contributions of the single-particle excitations and the plasmon excitation to the structure factor $\gamma_{ij}(q)$. The prime stands for the derivative with respect to ω. Some details about the limits of integration for the particle-hole continuum are discussed in Appendix B.

In FSC approximation, the iteration was started from the Hubbard expression for $G_{ij}(q)$ in Eq. (11); the equation $\mathrm{Re}\Delta(q,\omega)=0$ was then solved outside the particle-hole continuum to determine the plasma pole $\omega=\omega_p(q)$. $\gamma_{ij}(q)$ was computed from Eq. (51), which was then used to calculate $G_{ij}(q)$ in Eq. (50). In the second and subsequent iterations a mean of the previous G_{ij} and calculated G_{ij} was used to start the next iteration. Depending on the value of r_s, approximately 10 to 15 iterations were needed for a 0.1% or better convergence in $G_{ij}(q)$. This corresponds to much higher degree of accuracy in $\gamma_{ij}(q)$.

It may be mentioned here that the integral over q' in G_{ij} in Eq. (50) was calculated over the entire region from $q'=0$ to ∞. This was done by fitting $\gamma_{ij}(q')$ between $q'=10$ and 50 by a polynomial of the form $C_1/q'^4+C_2/q'^5+C_3/q'^6+\cdots$. The fit was then checked for $q'=70$ and 100 against the calculated values of $\gamma_{ij}(q')$. The fit was excellent. It was this polynomial that was used to calculate the integral $q'=10$ to infinity in Eq. (50). This is important for large q's as a substantial contribution to the integral in Eq. (50) comes from large values of q'. Having calculated $\gamma_{ij}(q)$, the partial-pair-correlation function $g_{ij}(r)$ and $\bar{\gamma}(r_s)$ were calculated from Eqs. (14) and (42) in a straightforward manner. To calculate the correlation energy from $\bar{\gamma}(r_s)$ we fit it to a suitable polynomial and evaluate the integral in Eq. (44). This procedure was repeated with several polynomials. The final accuracy of ϵ_{corr} is estimated to be better than $\frac{1}{4}\%$.

In SPH approximation with $G_{ii}(q)$ as given by Eq. (17), one only needs to solve one set of equations ($i=1$, $j=2$) to determine γ_{12} and G_{12} self-consistently. One can then calculate γ_{11} and γ_{22} from Eq. (51) using G_{ii} and self-consistent G_{12}.

In RPA and Hubbard approximations it is straightforward to evaluate Eq. (51) using $G_{ij}=0$ and Eq. (11), respectively, as there is no self-consistency involved.

In an ansiotropic situation the Lindhard function can be written[21]

$$Q^0_{i\,\text{elliptic}}(\vec{q},\omega)=(\tilde{q}^2/q^2)Q^0_{i\,\text{spherical}}(\tilde{q},\omega)\,, \tag{52}$$

where

$$\tilde{q}^2=\rho_i^{-1/3}[1+(\rho_i-1)\cos^2\theta]q^2\,, \tag{53}$$

$$\cos^2\theta=q_z^2/q^2,\quad \rho_i=m_{ti}/m_{li}\,,$$

and $Q^i_{0\,\text{spherical}}(\tilde{q},\omega)$ is the Lindhard function as given in Eqs. (48) and (49), with the important difference that here, in the definition of β_i, we must use the density-of-state mass m_{di}, Eq. (28), instead of the optical mass m_{oi} as used in the isotropic situation,

$$\beta_i=\mu/m_{di}\quad (m_i\equiv m_{di})\,.$$

The calculation in the Hubbard approximation remains straightforward as described above for the isotropic case. The appropriate expression for the local field G_{ii} in the anisotropic situation is given in Appendix C.

V. RESULTS AND DISCUSSION

A. Isotropic electron-hole liquid (model system)

Since the model system is free from all the complications of anisotropy of bands, it is amenable to a rigorous calculation within the framework of our approximation. We have calculated, in different approximations, the ground-state energy, enhancement factors, and partial-pair-correlation functions as a function of density r_s and mass ratio m_h/m_e. We shall discuss below our results for the model system in detail.

In Fig. 1 we have plotted the ground state energy per $e-h$ pair as a function of r_s in four different approximations for the mass ratio $m_h/m_e=1$. All four curves exhibit minima which lie between $r_s=1.90$ and 2.10. At the minimum the ground-state energy in the fully-self-consistent (FSC) approximation is nearly 15% lower than the corresponding value in the Hubbard approximation. In the FSC approximation the model system is not bound relative to free excitons.[39] The RPA gives a lower energy than the Hubbard approximation, which is not surprising, since it is known that RPA introduces too much correlation. One should also note that for a ground-state-energy calculation for small values of r_s ($r_s\leq 2$), the difference between the FSC and SPH approximations is small, the latter always overestimates the correlation energy. In a multi-component system such as normal Ge and Si, it is difficult at present, even on a big digital computer, to carry out a fully-self-consistent calculation, but a partial self-consistent SPH sol-

ution is possible. Fortunately, the difference between FSC and SPH approximations is very small in the region of interest of r_s values for Ge and Si. These systems will be discussed in a subsequent paper.

In Table III we have given the values of the correlation energy in different approximations for values of r_s in the range 0.2–4. The difference between the values in the Hubbard and FSC approximations steadily increases with the increase in r_s, becoming as much as 33% at $r_s=4$. It should be pointed out that our numerical values of the correlation energy in the Hubbard approximation agree to within 2% with those calculated by Brinkman and Rice.[21] Mathematically, within the Hubbard approximation our procedure and that of BR are exactly equivalent for $m_h/m_e=1$. For $m_h \neq m_e$, unlike BR, we do not make any further approximations. However, it turns out that numerically the differences are, indeed, very small.

As r_s increases beyond 4, the convergence of our fully-self-consistent numerical solution of the three coupled integral equations becomes slow and time consuming, and ultimately the scheme does not converge. In order to study the trend of the ground-state energy for $r_s>4$ and mass ratio unity, we have used the SPH approximation. The ground-state energy curve based on Hubbard approximation continues to rise and shows no tendency to bend and hence toward the formation of the excitonic state in the limit of large r_s. This is expected, since in the limit of large r_s it is the correlation energy alone which dominates and in that too it is the electron-hole contribution

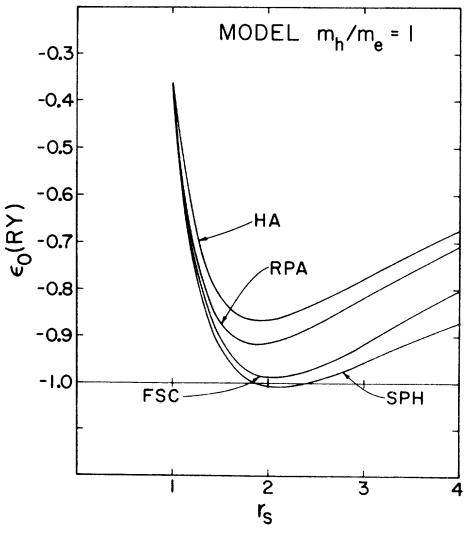

FIG. 1. Ground-state energy per e-h pair ϵ_0, in excitonic rydbergs, vs r_s in four approximations for the model system.

which is the largest, whereas the curve based on SPH approximation flattens out, and it shows no tendency even at $r_s=10$ to bend down and merge with the curve $\epsilon_0=-1$ Ry.

On the basis of the Mott criterion[40] for the metal-nonmetal transition, we should expect the formation of a bound excitonic state at $r_s \simeq 10$. Since the present theory fails to give a bound state, the obvious conclusion is that it is unsatisfactory in the limit of very low density. As in the calculation of positron annihilation rates[31] and correlation energy,[32] we feel that it is essential to use the expression for the local field $\psi(\vec{q})$ which involves the density-derivative terms[41] if we wish to push the fully-self-consistent calculation in the region of large r_s ($r_s>4$). Such a calculation is very time consuming and at present beyond our resources.

In Figs. 2 and 3 the partial-pair-correlation functions $g_{ee}(r)$ [for equal mass ratio $g_{ee}(r) = g_{hh}(r)$] and $g_{eh}(r)$ are plotted for $r_s=1$, and in Figs. 4 and 5 the same quantities are plotted for $r_s=2$. The first thing to note is that both RPA and HA give negative values for $g_{ee}(r)$ for small interparticle separations, which is not surprising. Another fact to note is that for $r_s=1$ the curves for $g_{ee}(r)$ in different approximations do not exhibit any structure except for very small Friedel oscillations (not seen in Figs. 2 and 3). On the other hand, for $r_s=2$, $g_{ee}(r)$ in, the FSC approximation exhibits marked oscillations, but the $g_{ee}(r)$ in

TABLE III. Correlation energy per e-h pair in excitonic rydbergs of the model system with $m_h/m_e=1$.

r_s	RPA ϵ_{corr}	Hubbard ϵ_{corr}	Self-consistent particle-hole ϵ_{corr}	Fully self-consistent ϵ_{corr}
0.2	−1.404	−1.288	−1.307	−1.293
0.4	−1.074	−0.982	−1.009	−0.993
0.6	−0.926	−0.845	−0.886	−0.867
0.8	−0.829	−0.755	−0.812	−0.793
1.0	−0.756	−0.689	−0.761	−0.742
1.2	−0.698	−0.636	−0.725	−0.706
1.4	−0.651	−0.593	−0.697	−0.678
1.6	−0.612	−0.557	−0.675	−0.657
1.8	−0.580	−0.528	−0.658	−0.639
2.0	−0.552	−0.502	−0.644	−0.624
2.2	−0.527	−0.480	−0.632	−0.609
2.4	−0.506	−0.461	−0.621	−0.595
2.6	−0.487	−0.443	−0.611	−0.581
2.8	−0.470	−0.428	−0.601	−0.566
3.0	−0.454	−0.413	−0.591	−0.552
3.2	−0.439	−0.400	−0.582	−0.537
3.4	−0.426	−0.388	−0.573	−0.522
3.6	−0.413	−0.376	−0.565	−0.508
3.8	−0.402	−0.366	−0.558	−0.495
4.0	−0.391	−0.356	−0.551	−0.484

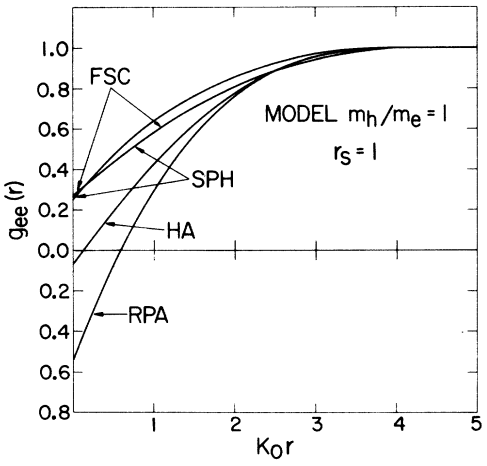

FIG. 2. Partial-pair-correlation function $g_{ee}(r)$ vs K_0r for the model system for $r_s = 1$.

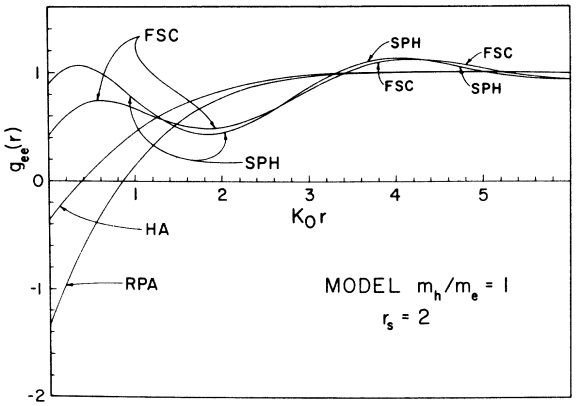

FIG. 4. Partial-pair-correlation function $g_{ee}(r)$ vs K_0r for the model system for $r_s = 2$.

both the RPA and Hubbard approximation is almost without any structure. This shows the importance of multiple scattering of electrons and holes with increasing r_s and the necessity of carrying out a self-consistent calculation. It is instructive to compare the curves for $g_{ee}(r)$ with those for $g_{eh}(r)$ (Figs. 4 and 5) for $r_s = 2$. For values of $K_0r \geq 2$, the maxima and minima in $g_{ee}(r)$ corresponding to Friedel oscillations have one-to-one correspondence with those in $g_{eh}(r)$, which is a manifestation of the fact that charge neutrality is almost maintained in any finite region of space.

In Figs. 6 and 7 are shown $g_{ee}(0)$ and $g_{eh}(0)$ as a function of r_s. For values of $r_s \leq 0.5$, it is seen that different approximations yield nearly the same values of $g_{eh}(0)$ as expected. Already, at $r_s = 2$, the effect of multiple scattering between electrons and holes is so large that the enhancement factor $g_{eh}(0)$ in the fully-self-consistent approximation is nearly three times the corresponding value in the Hubbard approximation. For values of $r_s > 4$, the convergence of the fully-self-consistent theory is extremely slow and one obtains very large enhancement factors indicating, as in the single positron case,[30,31] that the theory is breaking down. It should be recalled that in the definition used here (reduced mass) $r_s = 4$ corresponds to $r_s = 8$ in the electron-gas problem.

We have also calculated the ground-state energy for different values of mass ratio m_h/m_e as a function of r_s in the fully-self-consistent and Hubbard approximations. These results are shown in Fig. 8. For $m_h/m_e > 6$ the fully-self-consistent

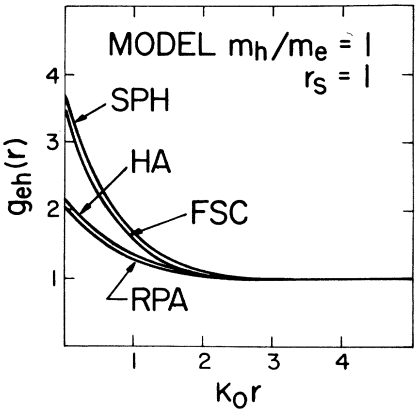

FIG. 3. Partial-pair-correlation function $g_{eh}(r)$ vs K_0r for the model system for $r_s = 1$.

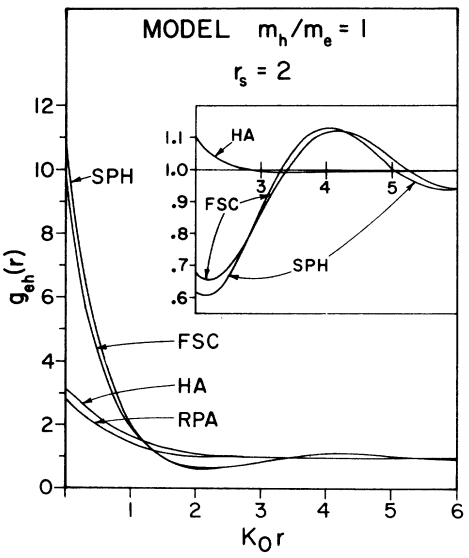

FIG. 5. Partial-pair-correlation function $g_{eh}(r)$ vs K_0r for the model system for $r_s = 2$.

theory converges very slowly, and hence no numerical results have been given. There are several points to note in Fig. 8: (i) In the FSC approximation one does not obtain a metallic binding, at least up to $m_h/m_e = 6$, and the value of the energy minimum almost remains constant with increasing m_h/m_e. (ii) In the Hubbard approximation one does obtain a metallic binding for $m_h/m_e > 10$. (iii) The r_s value at which the energy minimum occurs shifts slightly to lower values with increasing mass ratio m_h/m_e. In both the approximations the minimum occurs at nearly the same place. Assuming that this trend continues for larger mass ratios, one might conjecture that metallic hydrogen in the liquid phase might exist for r_s around 1.8.

In Table IV values of the correlation energy in Hubbard and FSC approximations are given for different values of r_s for mass ratios 2, 4, 6, and 10. Owing to slow convergence of the FSC scheme, we have calculated $\epsilon_{\rm corr}$ for $m_h/m_e = 4$ and 6 only up to $r_s = 2$; indeed, the approximation does not converge for $m_h/m_e \geq 10$ and $r_s \geq 2$.

In Figs. 9 and 10 are shown $g_{ee}(r)$ and $g_{hh}(r)$, respectively, for $r_s = 1$ and 2 for the mass ratio $m_h/m_e = 4$; in Figs. 11a and 11b are shown $g_{eh}(r)$ for $r_s = 1$ and 2, respectively. Here again there are several points to note: (i) On comparing Fig. 9 with Fig. 4, one sees that, in contrast to the case $m_h/m_e = 1$, $g_{ee}(r)$ for small values of r is positive for the mass ratio 4 in the Hubbard approximation for $r_s = 2$. Similarly, comparing Fig. 5 with Fig. 11(b), we see that the enhancement factor $g_{eh}(0)$ for mass ratio 4 is smaller than that in mass ratio unity for $r_s = 2$. This is simply due to the fact that although in the above two cases r_s is the same, the two systems actually correspond to different number densities, the latter being higher for mass ratio 4 than for mass ratio unity for a fixed r_s [see Eqs. (18) and (23)]. In the case of the enhancement factor $g_{eh}(0)$, the effect of increase of the hole mass is more than compensated by the increase in density. For a fixed density

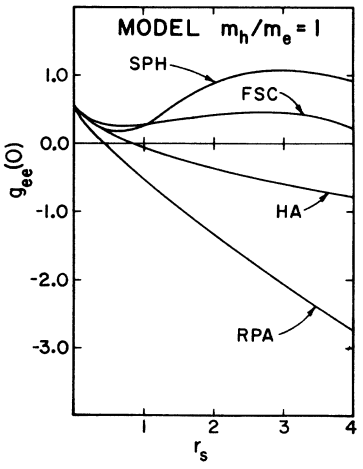

FIG. 6. $g_{ee}(r=0)$ vs r_s in four approximations for the model system.

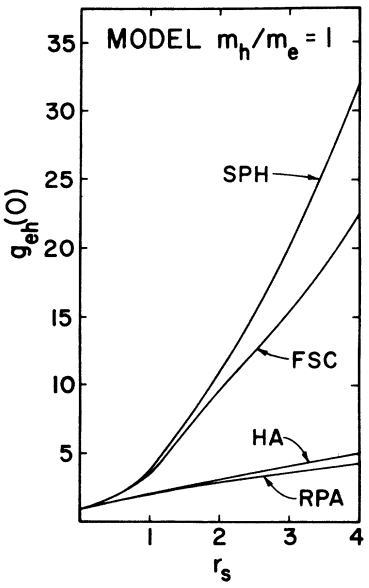

FIG. 7. $g_{eh}(r=0)$ vs r_s in four approximations for the model system.

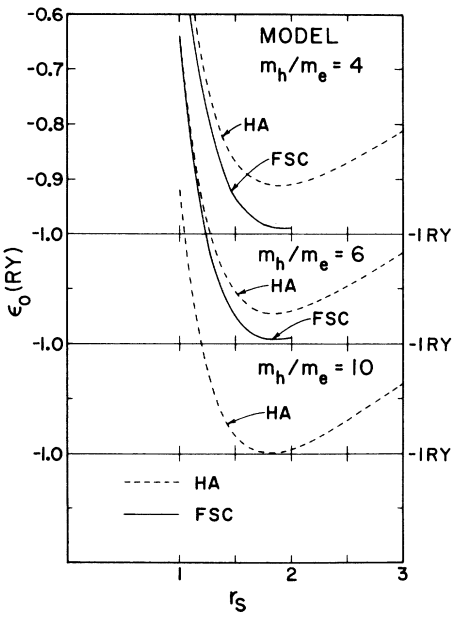

FIG. 8. Ground-state energy per e-h pair ϵ_0, in excitonic rydbergs, vs r_s in Hubbard and fully-self-consistent approximations for $m_h/m_e = 4$, 6, and 10. Note the shift in the vertical scale for the three cases.

TABLE IV. Correlation energy (isotropic) per e-h pair in excitonic rydbergs of the model system with mass ratios $m_h/m_e = 2$, 4, 6, and 10 in the Hubbard approximation (HA) and fully-self-consistent (FSC) approximation.

	$m_h/m_e = 2$		$m_h/m_e = 4$		$m_h/m_e = 6$		$m_h/m_e = 10$
r_s	HA	FSC	HA	FSC	HA	FSC	HA
0.2	−1.335	−1.335	−1.479	−1.463	−1.614	−1.576	−1.848
0.4	−1.013	−1.017	−1.107	−1.081	−1.196	−1.141	−1.348
0.6	−0.870	−0.886	−0.945	−0.935	−1.014	−0.978	−1.134
0.8	−0.776	−0.808	−0.840	−0.852	−0.898	−0.886	−0.996
1.0	−0.707	−0.756	−0.762	−0.793	−0.812	−0.822	−0.896
1.2	−0.652	−0.717	−0.701	−0.748	−0.745	−0.772	−0.819
1.4	−0.607	−0.688	−0.651	−0.710	−0.690	−0.729	−0.756
1.6	−0.571	−0.665	−0.609	−0.678	−0.645	−0.691	−0.705
1.8	−0.540	−0.645	−0.575	−0.650	−0.608	−0.657	−0.663
2.0	−0.513	−0.627	−0.546	−0.625	−0.577	−0.625	−0.627
2.2	−0.491	−0.611	−0.521		−0.550		−0.597
2.4	−0.471	−0.595	−0.500		−0.527		−0.571
2.6	−0.453	−0.579	−0.481		−0.506		−0.548
2.8	−0.437	−0.563	−0.463		−0.487		−0.527
3.0	−0.422	−0.547	−0.447		−0.470		−0.508

the enhancement factor always increases with the increase in hole mass. (ii) It is interesting to compare the enhancement factor in Fig. 11(b) with the enhancement factor for a proton in an electron gas.[31] In spite of the fact that the absolute number density here is lower than in the calculation of Ref. 31, and the reduced masses are not much different, the enhancement in Fig. 11(b) is still much smaller than that in the case of a proton in an electron gas. This is entirely due to the additional screening provided by the mobile holes in the electron-hole plasma. (iii) On comparison of Figs. 4 and 10, one notes that the exchange-correlation hole of $g_{hh}(r)$ is much deeper for mass ratio 4 than that for mass ratio unity. This is understandable since the kinetic energy of the hole for mass ratio 4 is much smaller than that for mass ratio unity.

In Figs. 12, 13, and 14 are shown, respectively, $g_{ee}(0)$, $g_{hh}(0)$, and $g_{eh}(0)$ as a function of r_s for different mass ratios in the Hubbard and FSC approximations. The Hubbard approximation gives large negative values for $g_{hh}(0)$ and as such cannot be trusted for large mass ratios. It is therefore not surprising that in this approximation the electron-hole plasma with mass ratio greater than 10 is bound relative to the free excitons.

In Figs. 15, 16, and 17 are plotted the local field corrections $G_{ee}(q)$, $G_{eh}(q)$, and $G_{hh}(q)$ for $r_s = 2$ for mass ratios 1 and 6 in various approximations. We might here recall the relation[25]

$$G_{ij}(q=\infty) = 1 - g_{ij}(r=0) .$$

In contrast to the electron-gas case, $G_{ee}(q)$ in the

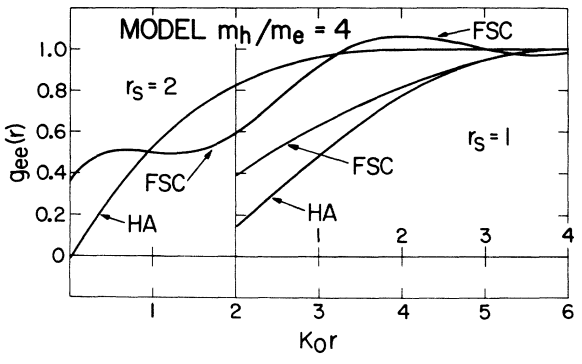

FIG. 9. Partial-pair-correlation function $g_{ee}(r)$ vs $K_0 r$ for the model system with mass ratio 4 for $r_s = 1$ and 2.

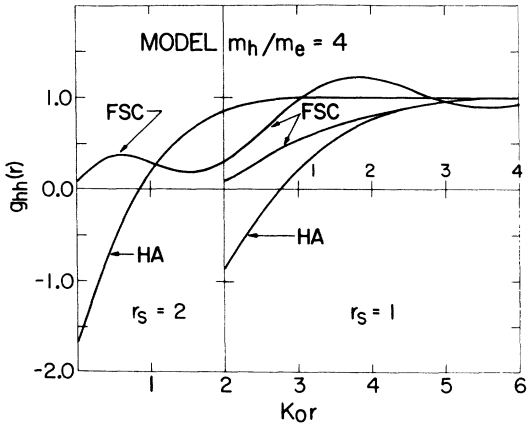

FIG. 10. Partial-pair-correlation function $g_{hh}(r)$ vs $K_0 r$ for the model system with mass ratio 4 for $r_s = 1$ and 2.

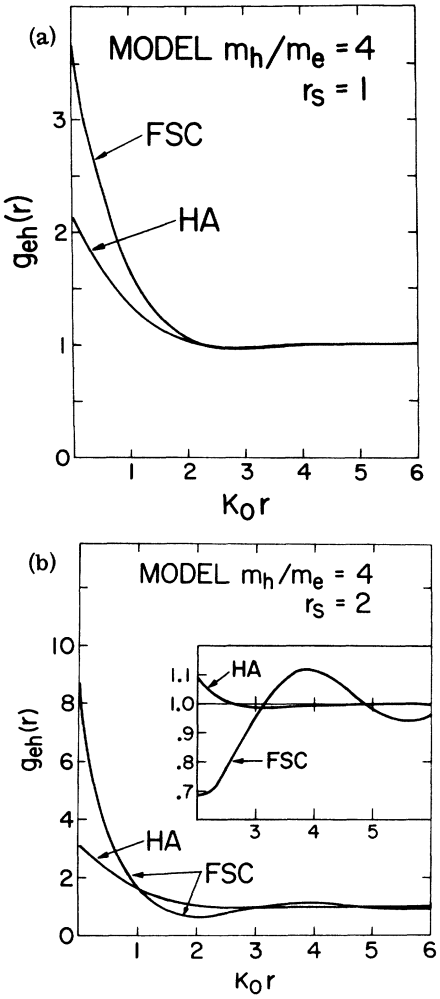

FIG. 11. (a) Partial-pair-correlation function $g_{eh}(r)$ vs $K_0 r$ for the model system with mass ratio 4 for $r_s = 1$. (b) Partial-pair-correlation function $g_{eh}(r)$ vs $K_0 r$ for the model system with mass ratio 4 for $r_s = 2$.

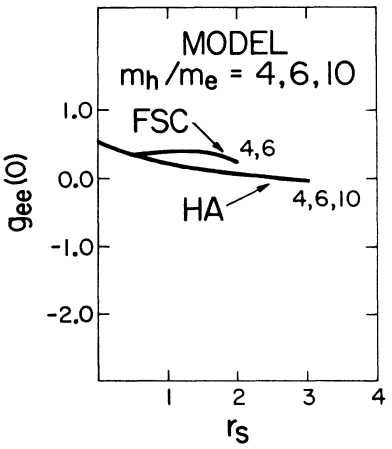

FIG. 12. $g_{ee}(r = 0)$ vs r_s for model system with mass ratio 4, 6, and 10.

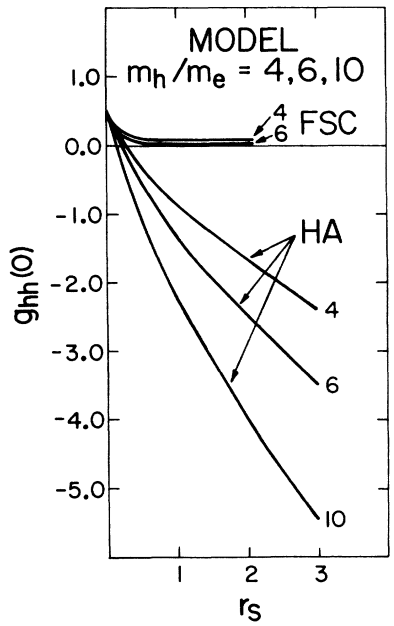

FIG. 13. $g_{hh}(r = 0)$ vs r_s for model system with mass ratio 4, 6, and 10.

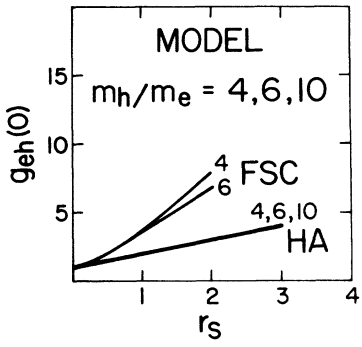

FIG. 14. Partial-pair-correlation function $g_{eh}(r = 0)$ vs r_s for model system with mass ratio 4, 6, and 10.

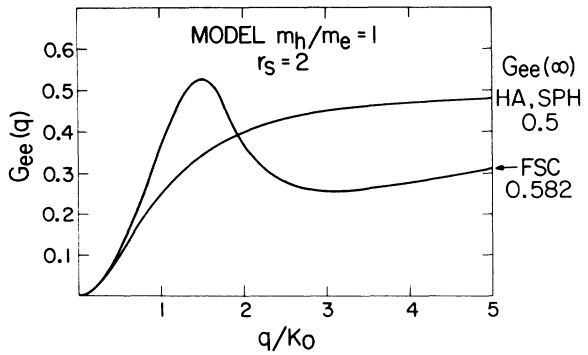

FIG. 15. Local field correction $G_{ee}(q)$ vs q/K_0 for the model system with $m_h/m_e = 1$ for $r_s = 2$. The values of $G_{ee}(q = \infty)$ in various approximations are also marked.

two-component plasma shows a structure in the fully-self-consistent theory. This structure is a manifestation of the structure in $g_{ee}(r)$. For $m_h/m_e=1$, $G_{hh}(q)$ is the same as $G_{ee}(q)$, whereas for $m_h/m_e=6$ (Fig. 17) $G_{hh}(q)$ has much more structure than $G_{ee}(q)$.

B. Anisotropic two-band system Ge[111]

In Fig. 18 the calculated ground-state energy per $e-h$ pair in germanium under a large uniaxial [111] stress is shown as a function of r_s in different approximations. Values of constants used in the calculation are given in Tables I and II. In the calculation of the correlation energy we have used the optically averaged masses[21] for electron and hole bands. Effects of anisotropy in the electron-hole bands have been fully taken into account in the Hartree-Fock energy contribution but *not* in the correlation-energy contribution.

It is again seen that compared to Hubbard approximation, RPA overestimates the ground-state energy. The difference between the values given by the curves marked HA and FSC gives an estimate of the contribution of multiple scattering. The latter at the energy minimum is 0.1 Ry. The system is bound relative to free excitons and the binding is largely due to multiple scattering. Taking the binding energy of an exciton[21] to be -1.002 Ry, we obtain the binding energy φ of the metallic phase to be 0.063 Ry = 0.167 meV. The energy minimum occurs at $r_s=1.67$, which corresponds to an equilibrium density $n_c=0.93\times10^{16}$ cm^{-3}.

In order to estimate the effect of anisotropy on the energy, we have calculated the correlation energy in the Hubbard approximation, including the effects of anisotropy of electron-hole bands. The difference in the values given by the curves marked HA (iso) and HA (aniso) in Fig. 19 gives us an estimate of anisotropy on the correlation

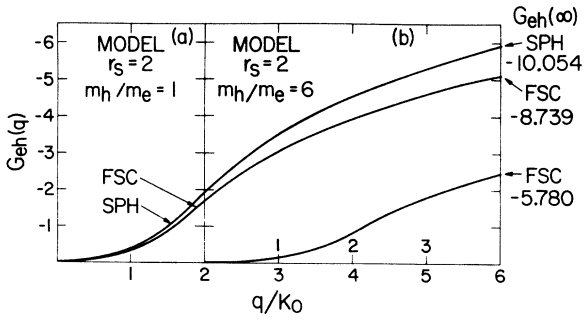

FIG. 16. (a) Local field correction $G_{eh}(q)$ vs q/K_0 for the model system with $m_h/m_e=1$ for $r_s=2$. (b) $G_{eh}(q)$ for the model system with $m_h/m_e=6$. The values of $G_{eh}(q=\infty)$ are marked.

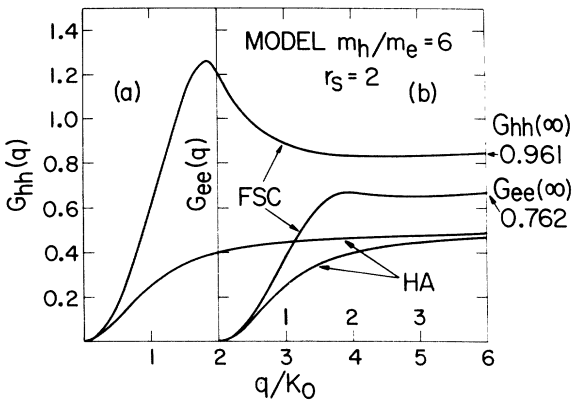

FIG. 17. (a) $G_{hh}(q)$. (b) $G_{ee}(q)$ vs q/K_0 for the model system with $m_h/m_e=6$ for $r_s=2$. Note the horizontal scale for $G_{hh}(q)$ and $G_{ee}(q)$. Values of $G_{hh}(q=\infty)$ and $G_{ee}(q=\infty)$ are marked.

energy in Hubbard approximation. This difference is then added to the fully-self-consistent value of the ground-state energy in the isotropic situation [FSC (iso) curve] to obtain the ground-state energy with anisotropy included fully. These values are shown by the curve marked FSC (aniso) in Fig. 19. Since the density dependence of the correlation energy is of some interest, we have in Table V given the values of ϵ_{corr}. In principle one can calculate the correlation energy with anisotropy included in

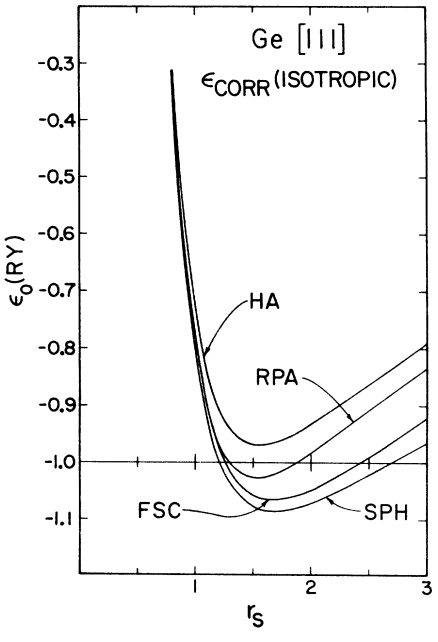

FIG. 18. Ground-state energy per e-h pair ϵ_0, in excitonic rydbergs, vs r_s in four approximations for Ge[111]. While the HF energy is exact here, ϵ_{corr} is calculated without anisotropy.

TABLE V. Correlation energy for Ge[111] and Si[100] in Hubbard and fully-self-consistent approximations.

	ϵ_{corr} Ge[111]				ϵ_{corr} Si[100]			
r_s	HA Isotropic	HA Anisotropic	FSC Isotropic	FSC Anisotropic	HA Isotropic	HA Anisotropic	FSC Isotropic	FSC Anisotropic
0.1	−1.831	−2.524	−1.850	−2.543	−2.278	−2.500	−2.279	−2.501
0.2	−1.310	−1.741	−1.313	−1.744	−1.617	−1.755	−1.618	−1.756
0.3	−1.109	−1.439	−1.111	−1.441	−1.357	−1.462	−1.360	−1.465
0.4	−0.995	−1.267	−1.000	−1.272	−1.206	-1.292	−1.214	−1.300
0.5	−0.916	−1.151	−0.927	−1.162	−1.101	−1.175	−1.116	−1.189
0.6	−0.856	−1.063	−0.874	−1.081	−1.021	−1.086	−1.044	−1.109
0.7	−0.807	−0.993	−0.833	−1.019	−0.956	−1.014	−0.989	−1.047
0.8	−0.765	−0.935	−0.800	−0.970	−0.902	−0.955	−0.946	−0.998
0.9	−0.729	−0.885	−0.772	−0.928	−0.856	−0.904	−0.911	−0.959
1.0	−0.697	−0.841	−0.749	−0.893	−0.815	−0.860	−0.882	−0.926
1.1	−0.669	−0.803	−0.729	−0.863	−0.780	−0.821	−0.857	−0.898
1.2	−0.643	−0.769	−0.711	−0.837	−0.748	−0.787	−0.836	−0.874
1.3	−0.620	−0.738	−0.695	−0.813	−0.720	−0.756	−0.817	−0.853
1.4	−0.599	−0.710	−0.682	−0.793	−0.695	−0.728	−0.800	−0.834
1.5	−0.580	−0.685	−0.669	−0.774	−0.671	−0.704	−0.784	−0.816
1.6	−0.563	−0.662	−0.658	−0.757	−0.650	−0.681	−0.769	−0.800
1.7	−0.547	−0.642	−0.648	−0.743	−0.631	−0.660	−0.754	−0.784
1.8	−0.532	−0.623	−0.639	−0.730	−0.613	−0.641	−0.740	−0.768
1.9	−0.519	−0.606	−0.630	−0.717	−0.597	−0.624	−0.726	−0.752
2.0	−0.506	−0.590	−0.622	−0.706	−0.582	−0.607	−0.712	−0.737
2.1	−0.495	−0.575	−0.614	−0.694	−0.567	−0.592	−0.697	−0.722
2.2	−0.484	−0.562	−0.607	−0.685	−0.554	−0.577	−0.683	−0.707
2.3	−0.474	−0.549	−0.600	−0.675	−0.541	−0.564	−0.669	−0.692
2.4	−0.465	−0.537	−0.592	−0.664	−0.529	−0.551	−0.656	−0.678
2.5	−0.456	−0.526	−0.585	−0.655	−0.518	−0.539	−0.643	−0.664
2.6	−0.448	−0.516	−0.578	−0.646	−0.507	−0.527	−0.630	−0.651
2.7	−0.440	−0.506	−0.571	−0.637	−0.497	−0.516	−0.618	−0.638
2.8	−0.432	−0.496	−0.564	−0.628	−0.487	−0.506	−0.608	−0.627
2.9	−0.425	−0.487	−0.557	−0.619	−0.478	−0.496	−0.598	−0.617
3.0	−0.418	−0.478	−0.549	−0.609	−0.469	−0.487	−0.590	−0.608

the FSC approximation, but the calculation is extremely time consuming. To make this calculation feasible we took recourse to the above-mentioned procedure—an approximation which seems reasonable. Thus with anisotropy included we obtain for the binding energy φ of the metallic phase with respect to the excitonic phase a value of 0.161 Ry = 0.426 meV and for the equilibrium density n_c corresponding to $r_s = 1.57$ a value of 1.11×10^{16} cm^{-3}. From Fig. 19 it is also clear that the effect of multiple scattering in Ge[111] is as large as the effect of anisotropy. One also notes that in the Hubbard approximation with isotropic e and h bands, one does not obtain any metallic binding. The enhancement factor $g_{eh}(0)$ corresponding to the equilibrium density is 6.8, whereas in the Hubbard approximation it is 2.6.

C. Anisotropic three-band system Si[100]

In Fig. 20 is shown the calculated ground-state energy with ϵ_{corr} (isotropic), per $e-h$ pair in Si under a large uniaxial [100] strain as a function of r_s in different approximations. The binding energy of the exciton has been taken to be 1.000 Ry.[42] It is interesting to note that with isotropic bands RPA gives metallic binding whereas the Hubbard approximation does not.

To estimate the effect of anisotropy we follow the same procedure as in the case of Ge[111]; the final results are shown in Fig. 21, which is self-explanatory. We obtain a binding energy φ for the metallic phase to be 0.146 Ry = 1.877 meV. The equilibrium density n_c corresponding to $r_s = 1.65$ is 4.47×10^{17} cm^{-3}. In Ge[111] the effect of anisotropy is of the same order as the effect of multiple scattering, whereas in Si[100] the latter is four times as large as the former.

The enhancement factor $g_{eh}(0)$ corresponding to the equilibrium density is 7.4, whereas in the Hubbard approximation it is 2.8.

V. CONCLUSION

From the foregoing comparative study of the ground-state energy of the quantum electron-hole liquid in the three cases (i) isotropic electron-hole liquid, (ii) Ge under a large [111] strain, and

(iii) Si under a large [100] strain under four different approximations, several interesting general conclusions emerge: (a) Compared to the Hubbard approximation, RPA, as a rule, always overestimates the ground-state energy. (b) In the region of large density, i.e., $r_s < 1$, the Hubbard approximation is satisfactory. (c) In the region of low density, i.e., $r_s > 1$, Hubbard approximation is poor and the effect of electron-hole multiple scattering is significant. (d) Although the difference in the correlation energy as given by the Hubbard and FSC approximations is not that large, the difference in the enhancement factors in the two approximations is indeed very striking. A relevant comparison here is between the density of electron at the hole in the metallic phase $3g_{eh}(0)/4\pi r_s^3$, and the density in the exciton wave function of π^{-1}. The ratio of these two for the model system with $m_e = m_h$ at the equilibrium density corresponding to $r_s = 2$ is 0.9 in the FSC approximation while it is only 0.3 in the Hubbard approximation.

In the case of the two interesting physical systems, Ge[111] and Si[100], investigated, our important results are summarized in Table VI. Both Ge and Si under a large uniaxial stress should exhibit metallized electron-hole droplets, and this transition to the metallic state in Si[100] is mostly due to the effect of electron-hole multiple scattering. In the case of Ge[111] the effect of

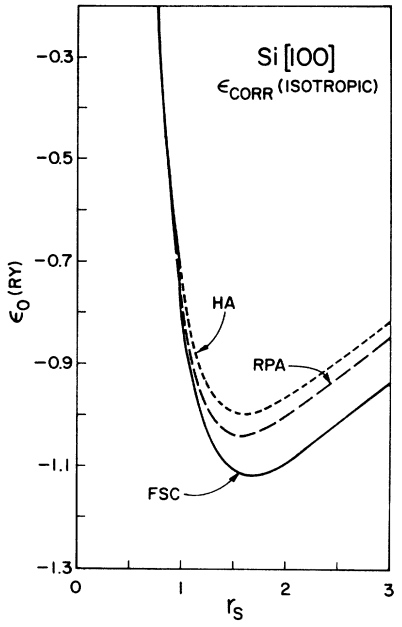

FIG. 20. Ground-state energy per e-h pair ϵ_0, in excitonic rydbergs, vs r_s in various approximations for Si[100]. While the Hartree-Fock energy is exact here, the correlation energy is calculated without anisotropy.

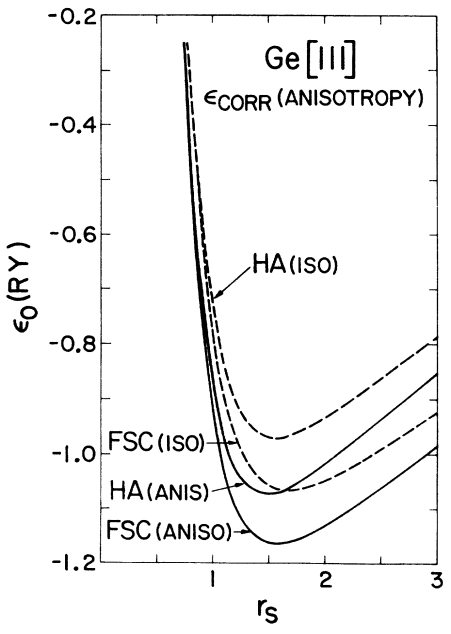

FIG. 19. Ground-state energy per e-h pair ϵ_0, in excitonic rydbergs, vs r_s for Ge[111]. Anisotropy is taken into account in ϵ_{corr}.

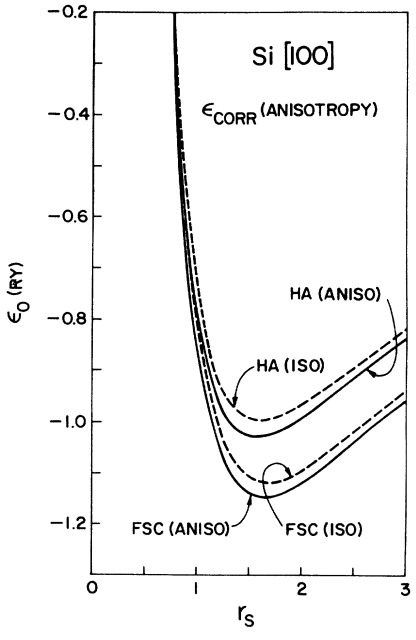

FIG. 21. Ground-state energy per e-h pair ϵ_0, in excitonic rydbergs, vs r_s for Si[100]. Anisotropy is taken into account in the correlation energy.

TABLE VI. A summary of results for the binding energy, ground-state energy, equilibrium density, and enhancement factor for Ge[111] and Si[100].

System	Binding energy[a] φ (°K)	Ground-state energy $-\epsilon_g$ (meV)	Critical density n_c (cm^{-3})	Enhancement factor $\rho \equiv g_{eh}(0)$
Ge[111]	4.9	3.08	1.11×10^{16}	6.8
Si[100]	21.8	14.73	4.47×10^{17}	7.4

[a] Note that the fundamental quantity here is the ground-state energy. The binding, $|\varphi|=\epsilon_g - \epsilon_{\text{exciton}}$, is subject to the value of the excitonic binding energy. We have taken $\epsilon_{\text{exciton}} = -2.655$ and -12.85 meV for Ge[111] and Si[100], respectively. When accurate experimental values of $\epsilon_{\text{exciton}}$ and dielectric constant κ are known then φ must be recomputed with them.

anisotropy is as important as the effect of multiple scattering. We get the binding energy of the metallic state in Si[100] to be 21.8 °K. This value is large enough that an experiment is feasible, and it would be indeed very interesting to perform such an experiment. Since the absolute value of the binding in Ge[111] (4.9 °K) is lower than in Si[100], the experiment in Ge[111] might pose additional difficulties.

In our view, experiments to establish quantatively the existence of a metallic phase in both highly strained Si[100] and Ge[111] are very important, since such experiments should be able to test different approximations of the many-body theory. In contrast to electrons in metals, we have here for the first time a system whose characteristics are known exactly. We hope that a way will be found to determine experimentally the enhancement factors, since they are very different in Hubbard and self-consistent approximations.

Note added in proof. Recently, P. Vashishta, S. G. Das, and K. S. Singwi [Phys. Rev. Lett. 33, 911 (1974)] have calculated the thermodynamics of the electron-hole liquid for five systems: Ge, Si, and Ge under large ⟨111⟩ uniaxial stress, Ge[111], Si under large ⟨100⟩ uniaxial stress, Si[100], and GaAs which is a direct band-gap semiconductor. Important effects of (e,e), (h,h), and (e,h) multiple scatterings and the anisotropy of the bands are included in the calculation of the correlation energy (FSC approximation with the effect of the anisotropy taken into account). For Ge, the ground-state energy, enhancement factor, compressibility, critical temperature, critical density, temperature dependence of Fermi energy, chemical potential, and equilibrium density are in good agreement with experiments. Predictions are made for other systems. In a recent experiment on Ge under uniaxial stress, T. Ohyama, T. Sanada, and E. Otsuka [Phys. Rev. Lett. 33, 647 (1974)] have found that the binding energy of the electron-hole liquid decreases as a function of the stress and the experiment seems to indicate that in the limit of large ⟨111⟩ uniaxial stress the binding energy tends toward a nonzero value.

ACKNOWLEDGMENTS

The authors wish to thank W. Kohn for correcting an important error and W. F. Brinkman and T. M. Rice for stimulating discussions.

APPENDIX A

In this appendix we write expressions for the response functions $\chi_{ij}(\vec{q},\omega)$ for a three-component plasma, as is the case for Si[100], in dimensionless form. We choose our notation such that the index 1 refers to holes whose density is n and 2 and 3 to the two equivalent conduction bands each of which has electron density $\frac{1}{2}n$.[36] We define

$$N_{ij}(\vec{q},\omega)\Delta^{-1}(\vec{q},\omega) = -\xi_i\xi_j\varphi(\vec{q})\chi_{ij}(\vec{q},\omega)\,, \tag{A1}$$

where $\xi_i = +1$ for holes and -1 for electrons and the $N_{ij}(\vec{q},\omega)$ corresponding to four independent correlation functions are

$$N_{11} = Q_1^0[(Q_2^0H_{22}+1)^2 - (Q_2H_{23})^2]\,, \tag{A2}$$

$$N_{22} = Q_2^0[(Q_1^0H_{11}+1)(Q_2^0H_{22}+1) - Q_1^0Q_2^0H_{12}^2]\,, \tag{A3}$$

$$N_{12} = Q_1^0Q_2^0[Q_2^0(H_{22}-H_{23})H_{12}+H_{12}]\,, \tag{A4}$$

$$N_{23} = -Q_2^{0\,2}[Q_1^0(H_{11}H_{23}-H_{12}^2)+H_{23}]\,, \tag{A5}$$

$$\Delta = \{(Q_1^0H_{11}+1)[(Q_2^0H_{23})^2 - (Q_2^0H_{22}+1)^2] + 2Q_1^0Q_2^0H_{12}^2[Q_2^0(H_{22}-H_{23})+1]\}\,, \tag{A6}$$

where $Q_i^0(\vec{q},\omega)$ is the Lindhard function as given in Eqs. (48) and (49) and

$$H_{ij}(\vec{q}) = 1 - G_{ij}(\vec{q})\,, \tag{A7}$$

where $G_{ij}(\vec{q})$ is defined in Eqs. (7) and (13). Equations (A1)–(A7) are analogs of Eqs. (45)–(47) for a two-component system.

In general, if the two conduction bands are not equivalent, the number of independent correlations will be six instead of four.

APPENDIX B

The imaginary part of the Lindhard function for the model system is

$$\begin{aligned} \mathrm{Im}Q_i^0(q,\omega) &= \text{finite} \quad \omega < (2q-q^2)\beta_i \ , \\ &= \text{finite} \quad |(2q-q^2)\beta_i| < \omega < (2q+q^2)\beta_i \ , \\ &= 0 \ , \quad \omega > (2q+q^2)\beta_i \ . \end{aligned} \tag{B1}$$

It is clear that, for the case of isotropic bands with $m_e = m_h$, single-particle excitation spectra for electrons and holes overlap for all q's. However, for the case of $m_h > m_e$, in principle there is a possibility that for some density we can have plasma poles along the dotted line in region II, as shown in Fig. 22. This is of course possible only if the plasma dispersion extends beyond $q = \bar{q}$, $\bar{q}$ is always greater than 2. However, in our calculations we have never found the plasma poles to extend beyond $q = 2$; for example, the plasma dispersion only extends up to $q = 1.45$ at $r_s = 4$ for the model system with $m_h = m_e$.

In the case of anisotropic bands, however, $\bar{q}$ can be less than 2. Care must then be exercised in making sure that if there are plasma poles in region II they should be taken into account. Even if one obtains a solution in the single-particle excitation region for ReΔ, it should not be considered as a genuine plasma pole, as its contribution is already included in the integral on the right-hand side of Eq. (52).

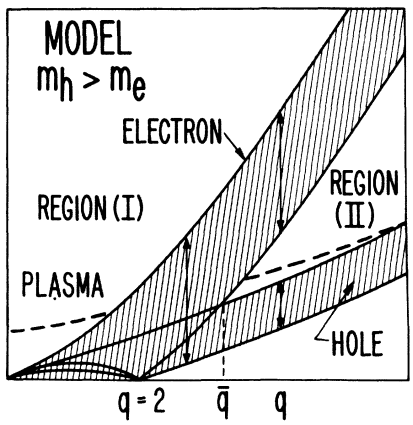

FIG. 22. Schematic diagram of the single-particle excitation spectra for the two-component plasma (model system $m_h > m_e$). At least one of the two Lindhard polarizabilities has nonzero imaginary part in the shaded region. ω and q are in units of $\hbar K_0^2/2\mu_0$ and K_0, respectively ($K_0 \equiv q_{Fe} \equiv q_{Fh}$).

In the case of a multicomponent plasma, since there are several polarizabilities, a careful examination of the single-particle spectra is required.

APPENDIX C: HUBBARD APPROXIMATION IN ELLIPTIC BANDS

For a two-component plasma the Hubbard approximation is obtained within the framework of the theory of Singwi *et al.* by inserting the Hartree-Fock (HF) structure factor in the expression for $G_{ii}(q)$ in Eq. (13). The HF structure factor is given by

$$\gamma_{ii}(q) = -\frac{2}{(2\pi)^3 n_i} \int_{\tau(\rho_i)} d\vec{k} \times \int_{\tau(\rho_i)} d\vec{k}' \, \delta(\vec{k} - \vec{k}' + \vec{q}) \ , \tag{C1}$$

where $\tau(\rho_i)$ defines the Fermi ellipsoid. Substituting Eq. (C1) in Eq. (13) for $G_{ii}(\vec{q})$, we have

$$G_{ii}(q) = \frac{2}{(2\pi)^6 n^2} \int_{\tau(\rho_i)} d\vec{k} \int_{\tau(\rho_i)} d\vec{k}' \, \frac{\vec{q}\cdot(\vec{k}-\vec{k}'+\vec{q})}{|\vec{k}-\vec{k}'+\vec{q}|^2} \ . \tag{C2}$$

From now on we shall drop the suffix i. In order to simplify Eq. (C2) we make the transformation

$$k_x = \rho^{1/6}\tilde{k}_x, \quad k_y = \rho^{1/6}\tilde{k}_y, \quad k_z = \rho^{-1/3}\tilde{k}_z \ , \tag{C3}$$

where $\rho = m_t/m_l$. Using the above transformation, we have

$$|\vec{k}-\vec{k}'+\vec{q}|^2 = \rho^{1/3}|\vec{\tilde{k}}-\vec{\tilde{k}}'+\vec{\tilde{q}}|^2[1+(\rho^{-1}-1)\mu^2] \ ,$$

where

$$\mu = (\vec{\tilde{k}}-\vec{\tilde{k}}'+\vec{\tilde{q}})\cdot\hat{z}/|\vec{\tilde{k}}-\vec{\tilde{k}}'+\vec{\tilde{q}}| \ . \tag{C4}$$

Following Hubbard we make the approximation

$$|\vec{\tilde{k}}-\vec{\tilde{k}}'+\vec{\tilde{q}}|^2 \simeq \tilde{q}_F^{\,2} + \tilde{q}^{\,2} \ , \tag{C5}$$

the assumption being that since $(\vec{\tilde{k}}-\vec{\tilde{k}}')$ goes over the entire Fermi surface, the average of $(\vec{\tilde{k}}-\vec{\tilde{k}}')\cdot\vec{\tilde{q}}$ is zero. Using Eq. (C5), $G_{ii}(\vec{q})$ can be rewritten

$$G_{ii}(\vec{q}) = \frac{2}{(2\pi)^6 n^2} \int_{\tau(\rho)} d\vec{\tilde{k}} \int_{\tau(\rho)} d\vec{\tilde{k}}' \times \left(\frac{\tilde{q}^{\,2}}{\tilde{q}^{\,2}+\tilde{q}_{\mathrm{Fi}}^{\,2}}\right) \frac{\rho^{1/3}[1+(\rho^{-1}-1)\mu'^2]}{\rho^{1/3}[1+(\rho^{-1}-1)\mu^2]} \ , \tag{C6}$$

where

$$\mu' = \hat{\tilde{q}}\cdot\hat{z} \ . \tag{C7}$$

For a given $\vec{\tilde{q}}$, the integral over μ in Eq. (C6) can be evaluated. However, in keeping with the

spirit of Hubbard approximation wherein, for large values of q, the form of local field is such that it cancels half the RPA contribution, one can see from Eqs. (C4) and (C7) that $\mu \to \mu'$, and hence Eq. (C6) takes the simple form

$$G(\tilde{q}) = \tfrac{1}{2}\tilde{q}^2/(\tilde{q}^2 + \tilde{q}_F^2) , \tag{C8}$$

where

$$\tilde{q}^2 = \rho^{-1/3}[1 + (\rho - 1)q_z^2/q^2] . \tag{C9}$$

---

*Work performed under the auspices of the U. S. Atomic Energy Commission, the Advanced Research Projects Agency of the Department of Defense through the Northwestern University Materials Research Center, and by the National Science Foundation under Contract No. GP-11054.

†Present address: Dept. of Physics, University of Illinois, Urbana, Illinois 61801.

[1]L. V. Keldysh, in *Proceedings of the Ninth International Conference on the Physics of Semiconductors, Moscow, 1968,* edited by S. M. Ryvkin and V. V. Shmastsev (Nauka, Leningrad, 1968), p. 1303.

[2]V. M. Asnin and A. A. Rogachev, Zh. Eksp. Teor. Fiz. Pis'ma Red. 9, 415 (1969) [JETP Lett. 9, 248 (1969)].

[3]Y. E. Pokrovsky and K. I. Svistunova, Zh. Eksp. Teor. Fiz. Pis'ma Red. 9, 453 (1969) [JETP Lett. 9, 261 (1969)].

[4]The first experimental observation of the shifted radiation in Si was by J. R. Haynes [Phys. Rev. Lett. 17, 860 (1966)]. His interpretation of the result was based on biexciton rather than the electron-hole plasma.

[5]Y. E. Pokrovsky and K. I. Svistunova, Fiz. Tekh. Poluprovodn. 4, 491 (1970) [Sov. Phys.-Semicond. 4, 409 (1970)].

[6]A. S. Kaminsky and Y. E. Pokrovsky, Zh. Eksp. Teor. Fiz. Pis'ma Red. 11, 381 (1970) [JETP Lett. 11, 225 (1970)].

[7]C. Benoît à la Guillaume, F. Salvan, and M. Voos, J. Lumin. 1, 315 (1970).

[8]Y. E. Pokrovsky, A. Kaminsky, and K. Svistunova, in *Proceedings of the Tenth International Conference on the Physics of Semiconductors, Cambridge, Massachusetts, 1970,* edited by S. P. Keller, J. Hensel, and F. Stern, CONF-700S01 (U. S. AEC Division of Tech. Information, Springfield, Va., 1970), p. 504.

[9]V. M. Asnin, A. A. Rogachev, and N. I. Sablina, Zh. Eksp. Teor. Fiz. Pis'ma Red. 11, 162 (1970) [JETP Lett. 11, 99 (1970)].

[10]C. Benoît à la Guillaume, M. Voos, F. Salvan, J. M. Laurant, and A. Bonot, C. R. Acad. Sci. B 272, 236 (1971).

[11]Y. E. Pokrovsky and K. I. Svistunova, Zh. Eksp. Teor. Fiz. Pis'ma Red. 13, 297 (1971) [JETP Lett. 13, 212 (1971)].

[12]For a more extensive list of references of Russian work, see the review article by Y. E. Pokrovsky [Phys. Status Solidi (A), 385 (1972)].

[13]C. Benoît à la Guillaume, M. Voos, and F. Salvan, Phys. Rev. B 5, 3079 (1972); C. Benoît à la Guillaume and M. Voos, Solid State Commun. 12, 1257 (1973).

[14]K. Betzler and R. Conradt, Phys. Rev. Lett. 28, 1562 (1972).

[15]J. C. Hensel, T. G. Phillips, and T. M. Rice, Phys. Rev. Lett. 30, 227 (1973).

[16]T. K. Lo, B. J. Feldman, and C. D. Jeffries, Phys. Rev. Lett. 31, 224 (1973).

[17]R. W. Martin and M. H. Pilkuhn, Solid State Commun. 11, 571 (1972).

[18]G. A. Thomas, T. G. Phillips, T. M. Rice, and J. C. Hensel, Phys. Rev. Lett. 31, 386 (1973).

[19]E. Hanamura in Ref. 8, p. 487; M. Inoue and E. Hanamura, J. Phys. Soc. Jpn. 34, 652 (1973).

[20]W. F. Brinkman, T. M. Rice, P. W. Anderson, and S. T. Chui, Phys. Rev. Lett. 28, 961 (1972).

[21]W. F. Brinkman and T. M. Rice, Phys. Rev. B 7, 1508 (1973).

[22]M. Combescot and P. Nozières, J. Phys. C 5, 2369 (1972).

[23]J. Hubbard, Proc. R. Soc. A 243, 336 (1957).

[24]P. Nozières and D. Pines, Phys. Rev. 111, 442 (1958).

[25]K. S. Singwi, M. P. Tosi, R. H. Land, and A. Sjölander, Phys. Rev. 176, 589 (1968); P. Vashishta and K. S. Singwi, Phys. Rev. B 6, 875 (1972) [Erratum Phys. Rev. B 6, 4883 (1973)].

[26]More recent estimates of the binding energy φ per e-h pair from luminescence data in Ge are (Thomas *et al.* Ref. 18), $1.98 \geq \varphi \geq 1.55$ meV and (Benoît à la Guillaume *et al.*, Ref. 13), 2 meV. The estimated thermodynamic value of φ is 1.54 ± 0.25 meV (Ref. 16). For Si the estimate of Benoît à la Guillaume *et al.* (Ref. 13) is 5.6 meV.

[27]C. Benoî à la Guillaume and M. Voos, Phys. Rev. B 7, 1723 (1973).

[28]V. S. Bagaev, T. I. Galkina, and O. V. Gogolin, in Ref. 8, p. 500.

[29]A brief account of this work was given by P. Vashishta, P. Bhattacharyya, and K. S. Singwi, Phys. Rev. Lett. 30, 1248 (1973). In this paper Si[100] is treated as a system consisting of one conduction and one valence band. Such a calculation leads to a binding energy of 11.3 K. In fact Si[100] consists of two equivalent conduction bands and one valence band. Clearly the ground-state energy for the three-component system will be lower than that of a two-component system because an increase in the number of components lowers the H-F energy, thus increasing the binding.

[30]A. Sjölander and M. J. Stott, Phys. Rev. B 5, 2109 (1972).

[31]P. Bhattacharyya and K. S. Singwi, Phys. Rev. Lett. 29, 22 (1972).

[32]P. Bhattacharyya and K. S. Singwi, Phys. Lett. A41, 457 (1972).

[33]D. Pines and P. Nozières, *The Quantum Theory of Liquids I* (Benjamin, New York, 1966), p. 95.

[34]J. Lindhard, Dan. Vidensk. Selsk. Mat.-Fys. Medd. 28, No. 8 (1954).

[35]P. Nozières, *The Theory of Interacting Fermi Systems* (Benjamin, New York, 1964), p. 36.

[36]J. C. Hensel and K. Suzuki, in Ref. 8, p. 541. For both Ge and Si the application of uniaxial stress lifts

the degeneracy between the valence bands at Γ. For a sufficiently large but readily attainable value of stress, the degeneracies are split by a sufficiently large amount that only one valence band need be considered. Ge: The four equivalent minima in the conduction band are ellipsoidal in shape and located at the L points of the zone. The application of a [111] stress raises the energy of the ellipsoids at other [111] points relative to the ellipsoid at the zone boundary in the direction of applied stress, and one is left ultimately with only one conduction band. Si: The six equivalent conduction minima are located at set of points obtained from $(0.85, 0, 0)2\pi/a$ so that under a large [100] stress four of the ellipsoids are raised, with two degenerate ellipsoids remaining behind. For details regarding the dispersion of the valence band under stress, see Table V of *Quantum Resonances in the Valence Bands of Germanium-Theoretical Considerations*. K. Suzuki and J. C. Hensel (to be published).

[37]D. Pines and P. Nozières, in Ref. 33, p. 296.

[38]R. A. Ferrell, Phys. Rev. Lett. 1, 443 (1958).

[39]For isotropic bands the Fermi surfaces of the electrons and the holes are identical and the system is unstable, at any density at zero temperature, toward the formation of e-h pairs. This instability has been discussed by several authors and arises from the divergence of the repeated e-h scattering diagrams in the metallic state. See, for instance, W. Kohn, in *Many-Body Physics*, edited by C. DeWitt and R. Bahan (Gordon and Breach, New York, 1968), p. 351, A. N. Kozlov and L. A. Maksimov, Zh. Eksp. Teor. Fiz. 48, 1184 (1965) [Sov. Phys.—JETP 21, 790 (1965)], and B. I. Halperin and T. M. Rice, Solid State Phys. 21, 115 (1968).

[40]N. F. Mott, Philos. Mag. 6, 287 (1961).

[41]P. Vashishta and K. S. Singwi (unpublished).

[42]W. Kohn and J. M. Luttinger, Phys. Rev. 97, 1721 (1955); Phys. Rev. 98, 915 (1955).